A Platinum Open Access Journal for Organic Chemistry

Paper

Free to Authors and Readers

DOAJ Seal

Arkivoc **2021**, part vi, 0-0

to be inserted by editorial office

The diffraction behavior of crystalline colloidal arrays formed by poly(styrene-co-sodium styrenesulfonate) particles

Caihua Ni,[a]* Ruili Wang,[b] Gwénaëlle Bazin,[b] Xiangjun Gong,[c] Geoffrey I. N. Waterhouse,[d] Armand Soldera,[e] and X. X. Zhu[b]*

[a]Institute of Polymer Chemistry, Nankai University, Tianjin, 300071, China; [b]Département de Chimie, Université de Montréal, C. P. 6128, Succursale Centre-ville, Montreal, QC, H3C 3J7, Canada; [c]Faculty of Materials Science and Engineering, South China University of Technology, Guangzhou, 510640, China; [d]School of Chemical Sciences, The University of Auckland, Auckland 1142, New Zealand; [e]Département de Chimie, Université de Sherbrooke, Sherbrooke, QC, J1K 2R1, Canada

E-mail: Julian.Zhu@umontreal.ca

This paper is dedicated to Professor Philip Hodge to commemorate his outstanding contribution to the field of polymer chemistry

Received 03-06-2021 **Accepted** 04-26-2021 **Published on line** 05-20-2021

Abstract

Colloidal particles were prepared by the surfactant-free emulsion copolymerization of styrene and sodium styrene sulfonate crosslinked with divinyl benzene. The mono-dispersed and highly surface-charged spherical particles self-assembled into three-dimensional crystalline colloidal arrays (CCA) in water. The CCA showed Bragg diffraction in the visible light wavelength range. Two diffraction peaks were observed in the range of 350~1000 nm for the CCAs at various particle concentrations. The two peaks shifted to longer wavelengths upon dilution of the colloids corresponding to increasing inter-particle distance. The red shift was accompanied by a gradual decrease in the intensity for the diffraction peak at the lower wavelength and an increase in the intensity of the peak at the higher wavelength.

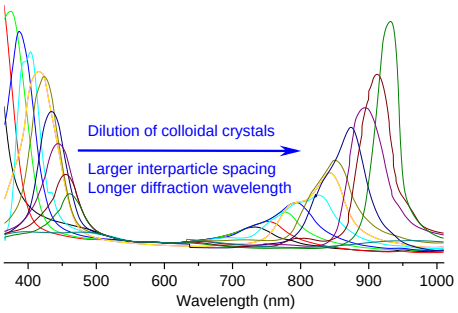

Keywords: Crystalline colloidal array; colloidal particles; Bragg diffraction

Introduction

Latex particles with high surface charges dispersed in water can self-assemble into ordered structures forming crystalline colloidal arrays (CCAs). Different methods have been developed to prepare CCAs for various purposes.[1-6] Such materials attracted interest for applications including optical devices (e.g., photonic band-gap materials),[7-10] genomics,[11] biosensors, and bio-separation.[12,13] The CCAs can diffract light in the range of UV-visible-near IR wavelengths according to Bragg's law. The understanding of the diffraction behavior is important for the design and use of such materials. Debord and Lyon prepared crystalline close-packed arrays based on poly (*N*-isopropylacrylamide) particles, and observed reversible order-disorder phase transition by studying its diffraction at different temperatures.[14] Hilter and Kriger studied Bragg diffraction of ordered suspension from polystyrene, and determined lattice parameters in ordered colloidal dispersions using the Bragg's equation.[15] They also studied the diffraction of ordered suspensions formed in non-aqueous solutions.[16] Asher and co-authors developed a series of sensing materials and device from polymerized crystalline colloidal arrays (PCCAs) with various chemical and biochemical sensing applications[17] to determine pH and ionic strength,[18] temperature,[30,31] glucose,[19,20] lead in bodily fluids,[21] metal ions,[22-24] creatinine in bodily fluids,[25] as well as recordable and erasable memories and/or display devices[26-28] and photonic crystal optical switches.[29]

In this work we prepared colloidal latex particles by emulsifier-free emulsion copolymerization of styrene (St) and sodium styrenesulfonate (NaSS). We have observed interesting diffraction patterns of the CCAs formed upon dilution.

Results and Discussion

The poly(St-co-NaSS) colloidal particles were prepared with the method similar to the procedure published by Sunkara et al.[32] and Zeng et al.[33] Uniform particles were obtained from this two-stage copolymerization method in a mixture of water and acetone and the particles packed well to form a CCA (Figure 1). The average diameter of the particles was determined to be 199 nm by dynamic light scattering (DLS) and 185 nm by scanning electron microscopy (SEM) (Figures 1 and 2), respectively. The slightly larger particle size obtained by DLS may be due to the hydrated state of the sample which has a viscous drag of a counterion shell around the colloidal particle in water.[32] The particles were uniform in size with a very narrow size dispersity of 0.005. The particles density was 1.06 g/cm^3 as determined by pycnometry and the surface charge density was 14.3 μc/cm^2 as measured by conductometric titration.

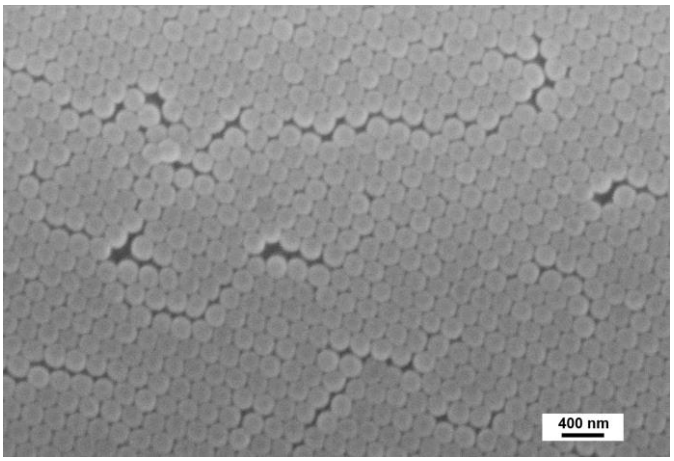

Figure 1. SEM image of the poly(St-co-NaSS) particles, showing their uniform size and crystalline packing.

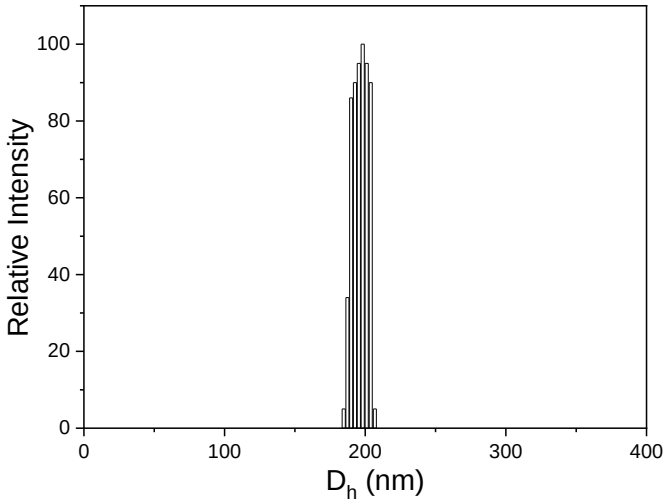

Figure 2. The distribution of the hydrodynamic diameter of the poly(St-co-NaSS) colloidal particles measured by DLS showing the narrow size distribution of the particles.

Variation of the diffraction wavelengths with particle concentration. Two diffraction peaks were observed for the CCA at various particle concentrations ranging from 3.10 to 9.30 wt% (Figure 3): One appeared in a shorter wavelength region (λ_1) and the other appeared at longer wavelengths (λ_2). For example, the CCA sample with particle concentration of 6.64 wt% showed two diffraction peaks with maxima at 374.8 and 775.3 nm, respectively, while the same sample at a particle concentration of 5.81 wt% showed two peaks at 388.0 and 796.9 nm. Although the observation of periodicity is common for X-ray diffraction of atomic and molecular crystals, the observation of more than one peak for CCAs is rather an exception. To the best of our knowledge, this observation of more than one peak has never been reported to date.

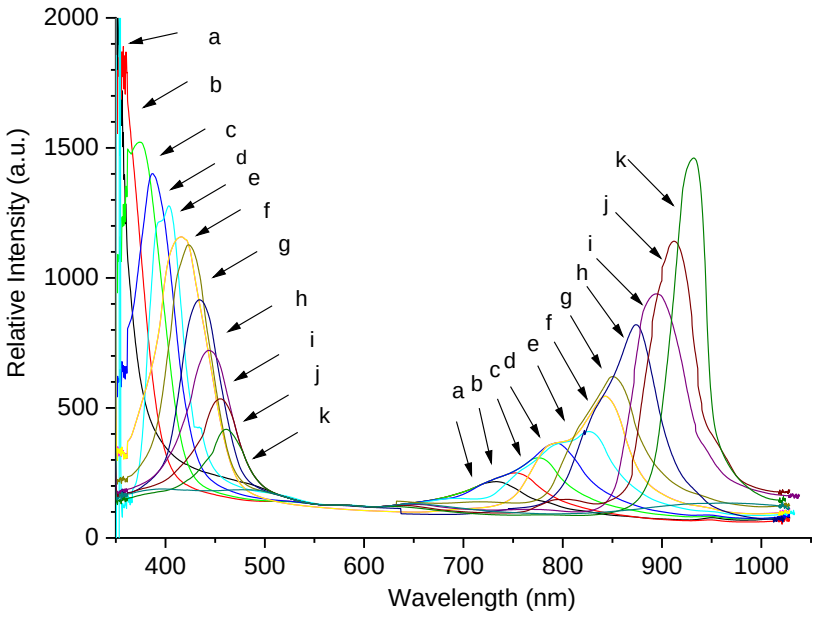

Figure 3. Diffraction patterns of the CCAs formed by the poly(St-co-NaSS) colloidal particles at different particle concentrations in water. (a) 9.30; (b) 7.75; (c) 6.64; (d) 5.81; (e) 5.17; (f) 4.65; (g) 4.23; (h) 3.88; (i) 3.58; (j) 3.32; (k) 3.10 wt%.

When the latex particle emulsion was diluted from 9.30 to 3.10 wt%, both diffraction peaks showed a gradual shift from shorter to longer wavelengths (Figure 3). According to Bragg's law

$$m\,\lambda = 2\,n\,d\,\sin\theta \qquad (1)$$

where m is the diffraction order, λ the diffraction wavelength, n the refractive index of the sample, and θ the angle between the incident light and the crystal planes. This red shift of the diffraction wavelength λ is caused by an increasing inter-particle distance d in the CCA upon dilution of the colloidal particles.

If we assume the formation of a cubic crystalline lattice for the CCA, for a sample of 100 mL in volume, the concentration of the colloidal particles can be expressed by

$$c = 100 / (d \times 10^{-7})^3 \times N \times 4/3\,\pi\,(r \times 10^{-7})^3\,\rho \qquad (2)$$

where c is the particle concentration (wt%), N the number of particles in a crystalline unit cell (N = 1, 2 and 4, respectively, for a simple cubic, body center cubic and face centered cubic cell), r and ρ are the radius (nm) and the density (g/cm^3) of the particles, respectively. When θ = 90° in the Bragg's equation (eq. 1), the lattice spacing can be calculated as $d = m\,\lambda / (2\,n)$. Since the variables r, n, ρ, and m in eq. 2 are all constants at a particular concentration of the particles, the particle concentration c can be re-written as

$$c = K\,N\,\lambda^{-3} \qquad (3)$$

where K is a constant at a certain colloidal particle concentration. Eq. 3 can be re-written as

$$\lambda = K N c^{-1/3} \qquad (4)$$

The data obtained fit perfectly to this relationship as shown in Figure 4A with correlation coefficients (r^2) of 0.999 and 0.998 for the two wavelengths λ_1 and λ_2, respectively. The results seem to validate the assumption of cubic lattice of the CCA and indicate that the two diffraction wavelengths showed proportional variation along with the dilution of the colloids.

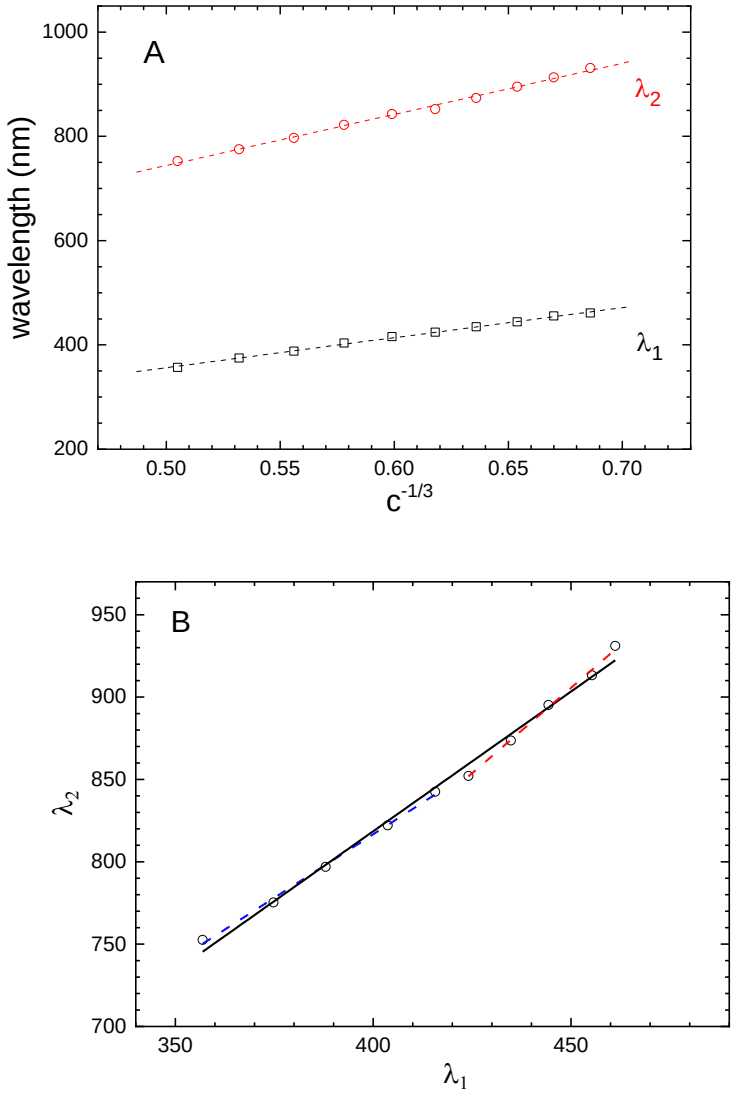

Figure 4. (A) The variation of the wavelengths of the two diffraction peaks (λ_1 and λ_2) with the colloidal particle concentration (wt%) in the CCAs formed by the poly(St-co-NaSS) colloidal particles, showing a liner relationship of λ with the with $c^{-1/3}$. (B) The variation of the wavelength of the second diffraction peak (λ_2) with that of the first (λ_1) give a good linear fit (slope = 1.70, r^2 = 0.993). The data may yield better linear fits for two separate wavelength ranges, one in the lower wavelength range (blue dashes, slope = 1.54, r^2 = 0.997) corresponding to the concentrated samples and the other in the higher wavelength range (red dashes, slope = 2.08, r^2 = 0.995) corresponding to the relatively dilute samples.

The plot of the wavelengths of the two diffraction peaks in Figure 4B also shows a very good linear relationship, but the slope is ca. 1.70, lower than an integer of 2 expected for the diffraction order *m* in eq. 1. A closer analysis of the data shows that better linear fits may be obtained for the lower and higher wavelength ranges separately, corresponding to the more and less concentrated samples, respectively. In the lower concentration range (higher wavelengths), the slope (2.08) is closer to 2 and reduces to ca. 1.54 for the higher concentration range (lower wavelengths). It is possible that well-ordered colloidal crystals form in solution at low colloid concentrations, although the colloidal particles do not touch each other due to the high surface charge on the individual particles. Hence the solid volume fraction in the colloidal crystals is much less than 0.74 and the interlayer spacing (*d*) between the layers of colloids causing the diffraction is large. Therefore, both diffraction peaks are observed at higher wavelengths since both λ_1 and λ_2 are directly proportional to the interlayer spacing (*d*).

Variation of the diffraction intensities with particle concentration. In addition to the red shifts of the diffraction peaks, the peak intensities also showed systematic changes in the opposite direction along with the dilution of the CCA formed by the colloidal particles. As shown in Figure 3, the first peak at λ_1 on the left side of the diffraction patterns gradually decreased in intensity along with some broadening of the peak, while the second peak at λ_2 increased in intensity and became sharpened. The variations of the peak intensity are shown in Figure 5A and the relationship of the intensities of the two peaks are shown in Figure 5B. The results seem to indicate that the two peaks are not exactly results of a diffraction order (as shown in Figure 4B). The diffraction order *m* in eq. 1 should have been an integer and the two peaks should have shown proportional intensities. Based on these observations, it appears that two phases or two kinds of lattices may have co-existed in the sample, both meeting the Bragg's diffraction condition. In Figure 4A, the line with λ_2 has a sharper slope (9.81×10^2) than the line with λ_1 (5.77×10^2), indicating that these two peaks may represent two different crystalline lattices. According to eq. 4, a larger slope corresponds to a larger N value, which may be a sign of a transition from simple cubic to body center cubic then to face center cubic lattices. It is difficult, however, to imagine or understand a transition from a looser packing to a closer packing with the dilution of the particles. We speculate that the intensity changes resulted probably from the changes of packing order on the surface layer or from the observable number of lattices in the CCAs since diffraction intensity is a function of lattice number according to the diffraction theory. The diffraction maintains a good pattern even for diluted mixtures, possibly due to the stability provided by the long-distance electrostatic repulsive forces since the colloidal particles are highly charged on the surface. It seems that relatively well-ordered CCAs formed at low colloid concentrations. At high colloid concentrations, the charged colloids are forced to interact more with each other. This decreased the interlayer spacing between the layers of colloids, corresponding to the shift of the diffraction peaks to shorter wavelengths (Figure 3). The individual colloid layers became more disordered as the colloid concentration increased due to the charge on the colloids, which caused the changes in the width and intensity of the diffraction peaks.

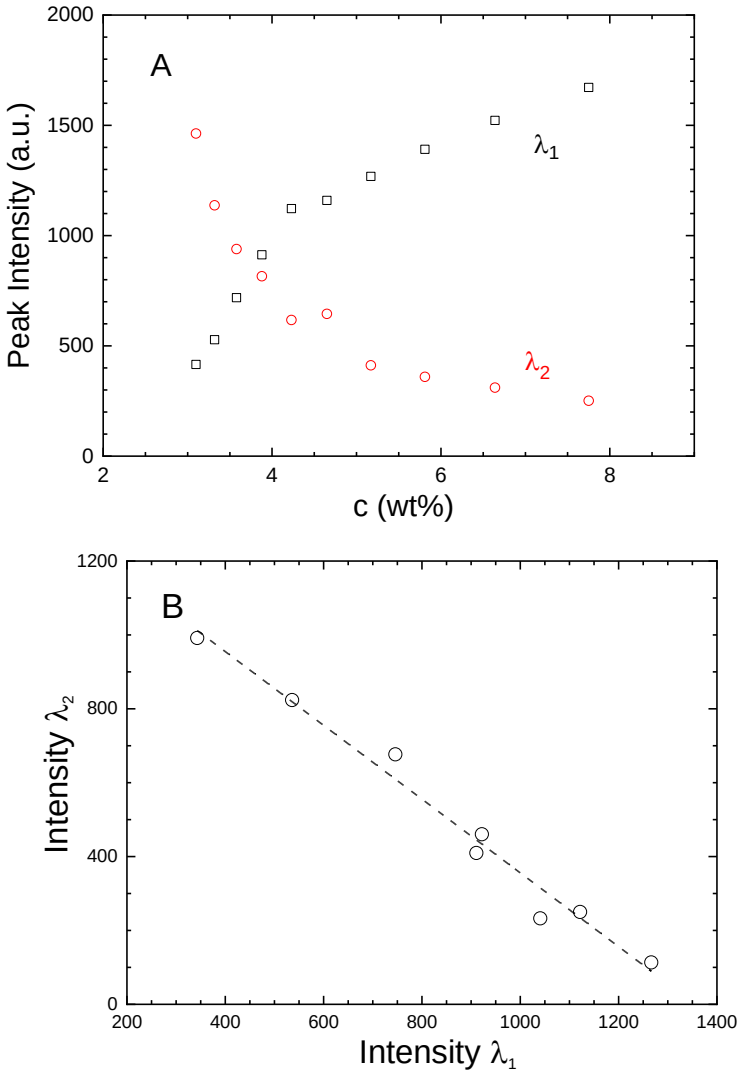

Figure 5. (A) The variation of the intensities of the maxima λ_1 (black squares) and λ_2 (red circles) of the two diffraction peaks with the concentration of the poly(St-co-NaSS) colloidal particles in the CCAs (wt%). (B) The linear relationship of the intensities of the two diffraction peaks showing a slope of -0.999 (r^2 = 0.978).

Conclusions

We report for the first time the observation of two diffraction peaks in the wavelength range of 350~1000 nm of the CCAs formed by the highly surface-charged uniform-sized poly(St-co-NaSS) spherical particles. The wavelengths of the two peaks increase with the dilution of the colloidal particles due to the increased inter-particle distance according to Bragg's law of diffraction. The opposite change of the intensities of the two diffraction peaks upon dilution seems to indicate the transition from one crystalline phase to another, but it is rather hard to explain. In fact, it is possibly related to the changes of observable number of crystalline lattices in the CCAs. Further investigation may be needed to gain a better understanding of this interesting and rare

diffraction behavior, most likely with other particles than the polymeric ones since it is not easy to precisely control the colloidal particle size with emulsion polymerization techniques.

Experimental Section

General. Sodium styrenesulfonate (NaSS) and potassium persulfate (PPS) were purchased from Aldrich. Styrene (St) and divinyl benzene (DVB) were purchased from Tianjin Chemical Company. St was re-distillated under reduced pressure, and the other chemicals were used as received without further purification.

Colloidal particle preparation. The poly(St-co-NaSS) particles were synthesized by emulsifier-free emulsion polymerization. A 250 mL of 4 neck round-bottom flask was fitted with mechanical stirrer, thermometer, condenser, and nitrogen inlet. The flask was charged with 130 mL ultrapure water, 13.5 g St, 0.1 g NaSS, 0.2 g DVB, and 0.07 g $NaHCO_3$, and the mixture was bubbled with nitrogen for 20 min. After the addition of acetone (15 mL) and the initiator PPS (0.2 g in 5 mL water), the polymerization was carried out for 3 h at 70 °C. The second batch of reactants (2.4 g St, 0.45 g NaSS, 0.04 g DVB, 0.02 g $NaHCO_3$) was added, and the reaction continued for 4 h. The white colloidal particles obtained were filtered through wool and the filtrate was washed with 0.5 N HCl and centrifuged into a pellet, and the supernatant was removed. The particles were washed with ultrapure water through a process of repeated centrifugation and re-dispersion by sonication (three times, or until a diffraction pattern can be observed). The colloidal latex was dialyzed against ultrapure water which was replaced daily for 3 days. For storage, mixed anionic and cationic ion exchange resins were added to the colloidal particles.

The diameters of the particles were measured by DLS and SEM. The surface charge density was determined by conductometric titration. A standard NaOH solution (0.01 M) was used to titrate 25 mL of the colloidal particles. The polymer content of the latex (weight percentage of the solid) was determined by weighing the samples when they are dried at 110 °C to a constant weight. The polymer density was determined by pycnometry.

Diffraction of the CCAs. One milliliter of the colloidal particles was placed in a quartz cell (1 × 1 × 5 cm) and was kept still for 1 h for the formation of a stable CCA. The diffraction was measured with USB200 spectrometer (R200-7VIS/NIR 350~1000 nm, LS-1 tungsten light source, Ocean Optics, USA). The probe of the instrument was placed in contact with the outside wall of the cell for the recording of the diffraction peaks. For the gradual dilution, ultrapure water (0.2 mL each time) was added to the cell followed by vigorous shaking for a few minutes. The cell was then kept static for the formation of a stable CCA and the recording of the diffraction pattern.

Acknowledgements

Financial support of this work from NNSFC and NSERC is acknowledged. Authors from Université de Montréal and Université de Sherbrooke are members of Quebec Center for Advanced Materials funded by FRQNT.

References

1. Zheng, H.; Ravaine, S. *Crystals* **2016**, *6*, 54-78. https://doi.org/10.3390/cryst6050054
2. García Núñez, C.; Taube Navaraj, W.; Liu, F.; Shakthivel, D.; Dahiya, R. *ACS Appl. Mater. Interfaces* **2018**, *10*, 3058-3068. https://doi.org/10.1021/acsami.7b15178
3. Greybush, N.J.; Liberal, I.; Malassis, L.; Kikkawa, J.M.; Engheta, N.; Murray, C.B.; Kagan, C.R. *ACS Nano*. **2017**, *11*, 2917-2927. https://doi.org/10.1021/acsnano.6b08189
4. Ye, X.; Huang, J.; Zeng, Y.; Sun, L.-X.; Geng, F.; Liu, H.-J.; Wang, F.-R.; Jiang, X.-D.; Wu, W.-D.; Zheng, W.-G.. *Nanomaterials*. **2017**, *7*, 291-301. https://doi.org/10.3390/nano7100291
5. Parker, R.M.; Guidetti, G.; Williams, C.A.; Zhao, T.; Narkevicius, A.; Vignolini, S.; Frka-Petesic, B. *Adv. Mater.* **2018**, *30*, 1704477-1704489. https://doi.org/10.1002/adma.201704477
6. Zhang, X.; Yu, L.; Zhang, W.; Hu, F.; Wang, Y. *J. Crystal Growth*. **2019**, *508*, 82-89. https://doi.org/10.1016/j.jcrysgro.2018.12.031
7. Vlasov, Y.A.; Yao, N.; Norris, D.J. *Adv. Mater.* **1999**, *11*, 165-169. https://doi.org/10.1002/(SICI)1521-4095(199902)11:2<165::AID-ADMA165>3.0.CO;2-3
8. Subramania, G.; Constant, K.; Biswas, R.; Sigalas, M.; Ho, K.M. *App. Phys. Lett.* **1999**, *74*, 3933-3935. https://doi.org/10.1063/1.124228
9. Pan, G.S.; Kesavamoorthy, R.; Asher, S.A. *J. Am. Chem. Soc*. **1998**, *120*, 6525-6530. https://doi.org/10.1021/ja980481a
10. Vos, W.L.; Sprik, R.; Vanblaaderen, A. Imhof, A.; Lagendijk, A.; Wegdam, G.H. *Phys. Rev. B: Condens. Matter. Phys*. **1996**, *53*, 16231-16235. https://doi.org/10.1103/PhysRevB.53.16231
11. Storhoff, J.J.; Elghanian, R.; Mucic, R.C.; Mirkin, C.A.; Letsinger, R.L. *J. Am. Chem. Soc.* **1998**, *120*, 1959-1964. https://doi.org/10.1021/ja972332i
12. Lyon, L.A.; Musick. M.D.; Natan, M. *J. Anal. Chem.* **1998**, *70*, 5177-5183. https://doi.org/10.1021/ac9809940
13. Liu, L.; Li, P.S.; Asher, S.A. *Nature* **1999**, *397*, 141-144. https://doi.org/10.1038/16426
14. Debord, J.D.; Lyon, L.A. *J. Phys. Chem. B.* **2000**, *104*, 6327-6331. https://doi.org/10.1021/jp001238c
15. Hilter, P.A.; Kriger, I.M. *J. Phys. Chem. B.* **1969**, *73*, 2386-2389. https://doi.org/10.1021/j100727a049
16. Hilter, P. A.; Papair, Y.S.; Kriger, I.M. *J. Phys. Chem. B.* **1971**, *75*, 1881-1886. https://doi.org/10.1021/j100681a020
17. Asher, S.A.; Holtz, J.; Liu, L.; Wu, Z. *J. Am. Chem. Soc.* **1994**, *116*, 4997-4998. https://doi.org/10.1021/ja00090a059
18. Lee, K.; Asher, S. A. *J. Am. Chem. Soc.* **2000**, *122*, 9534-9537. https://doi.org/10.1021/ja002017n
19. Alexeev, V.L.; Sharma, A.C. Goponenko, A.V.; Das, S.; Lednev, L.K.; Wilcox, C.S.; Finegold, D.N.; Asher, S.A.

Anal. Chem. **2003**, *75*, 2316-2323.
https://doi.org/10.1021/ac030021m
20. Asher, S.A.; Alexeev, V.L.; Goponenko, A.V.; Sharma, A.C.; Lednev, L.K.; Wilcox, C.S.; Finegold, D.N. *J. Am. Chem. Soc.* **2003**, *125*, 3322-3329.
https://doi.org/10.1021/ja021037h
21. Asher, S.A.; Peteu, S.F.; Reese, C.E.; Lin, M.X.; Finegold D. *Anal. Bioanal. Chem.* **2002**, *373*, 632-638.
https://doi.org/10.1007/s00216-002-1366-z
22. Asher, S.A.; Sharma, A.C.; Goponenko, A.V.; Ward M.M. *Anal. Chem.* **2003**, *75*, 1676-1683.
https://doi.org/10.1021/ac026328n
23. Holtz, J. H.; Holtz, J. S. W.; Munro, C. H.; Asher, S. A. *Anal. Chem.* **1998**, *70*, 780-791.
https://doi.org/10.1021/ac970853i
24. Geary, C.D.; Zudans, I.; Goponenko, A. V.; Asher, S.A.; Weber, S.G. *Anal. Chem.* **2005**, *77*, 185-192.
https://doi.org/10.1021/ac048616k
25. Sharma, A.C.; Jana, T.; Kekavamoorthy, R.; Shi, L.; Virji, M.A.; Finegold, D.N.; Asher, S.A. *J. Am. Chem. Soc.* **2004**, *126*, 2971-2977.
https://doi.org/10.1021/ja038187s
26. Kamenjiki, M. *Macromolecules* **2004**, *37*, 8293-8296.
https://doi.org/10.1021/ma049678f
27. Kamenjiki, M.; Lednev, I.K.; Mikhonin A.; Kesavamoorthy, R.; Asher, S.A. *Adv. Funct. Mater*. **2003**, *13*, 774-780.
https://doi.org/10.1002/adfm.200304424
28. Kamenjiki, M.; Lednev, I.K.; and Asher, S.A. *J. Phys. Chem. B* **2004**, *108*, 12637-12639.
https://doi.org/10.1021/jp047500p
29. Reese, C.E.; Mikhonin, A. V.; Kamenjicki, M.; Tikhonov A. and Asher, S.A. *J. Am. Chem. Soc*. **2004**, *126*, 1493-1496.
https://doi.org/10.1021/ja037118a
30. Weissman, J.M.; Sunkara, H.B.; Tse, A.S.; Asher, S.A. *Science* **1996**, *274*, 959-960.
https://doi.org/10.1126/science.274.5289.959
31. Reese, C. E.; Baltusavich, M. E.; Keim, J. P.; Asher, S. A. *Anal. Chem*. **2001**, *73*, 5038-5042.
https://doi.org/10.1021/ac010667j
32. Sunkara, H.B.; Jethmalani, J.M.; Ford, W.T. *J. Polym. Sci.: Part A: Polym. Chem.* **1994**, *32*, 1431-1435.
https://doi.org/10.1002/pola.1994.080320804
33. Zeng, F.; Sun, Z.; Wu, S.; Liu, X.; Wang, Z.; Tong, Z. *Macromol. Chem. Phys*. **2002**, *203*, 673-677.
https://doi.org/10.1002/1521-3935(20020301)203:4<673::AID-MACP673>3.0.CO;2-S